Features of Free Motion Persist in Constrained Actions

James Hermus, Dagmar Sternad, and Neville Hogan

I. Introduction

Despite large feedback delays, humans excel at physical interaction with complex objects. Nonetheless, neuroscience research has primarily focused on the examination of unconstrained motions. To search for fundamentals which underlie human physical interaction, we developed an upper limb crank turning experiment.

One widely observed pattern in unconstrained movement trajectories is that velocity systematically scales with curvature in the so-called "2/3 power law" [1]. The 2/3 power is exact in simple curves such as an ellipse. In more complex curves the power changes, but all shapes show a coincidence between velocity and curvature extrema [2], [3]. This power law relation is ascribed to neural control, and has been observed in isometric tasks where subjects managed force to move a virtual point [4], and in monkey motor cortical activity [5]. However, alternative interpretations were reported [6].

Motion under a circular constraint (i.e. turning a crank) imposes constant curvature of the hand path and hence does not require variations of speed. However, constrained motion also includes forces against the constraint, implying a zero-force trajectory (defined below) that is not circular and does not show constant speed. We will determine the zero-force trajectory and **hypothesize that the power law relation will persist if this relation is of neural origin**.

II. Methods

Ten right handed subjects turned a crank (radius 10 cm) in two directions (clockwise and counterclockwise), and in three speed conditions (slow (0.075 rev/s), medium (0.5 rev/s), and fast (2 rev/s)). Visual velocity feedback was provided on a display. Subjects completed 23 trials in each condition.

Because kinematically-constrained actions necessarily involve significant physical interaction, disentangling the influences of biomechanics and neural control is a challenge. We assumed a plausible mathematical model of interactive dynamics and used it to 'subtract off' or 'peel back' peripheral biomechanics, revealing underlying neural influence expressed in terms of motion. We called this quantity the zero-force trajectory – this computation is explained in the appendix.

For each local minimum in tangential speed of the zero-force trajectory, the nearest local maximum in curvature of the zero-force trajectory was found. The signed distance between the two extrema was normalized by the target speed, and defined as the interval, Δ. This was computed for each subject in each condition, and the data were pooled across trials. The 95% confidence interval for each subject in each condition was computed.

III. Results

Figure 1b is a representative plot of the zero-force trajectory for the circular constraint. Clearly, the zero-force trajectory systematically deviates from the circular constraint (dashed line) showing an elliptic shape. The color coding illustrates how the velocity decreased as the curvature increased. Figure 2a shows tangential velocity vs. angle illustrating the coincidence of extrema in velocity and curvature. Figure 2b summarizes these findings in a histogram of Δ. The interval Δ often slightly led or lagged zero. Nonetheless, all 95% confidence intervals for Δ were less than 3% of a revolution from zero.

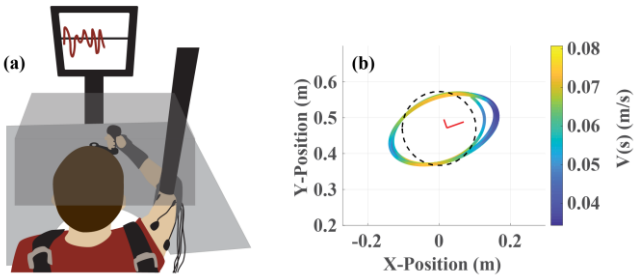

Figure 1: (a) A mechanical crank was used to provide a circular constraint. The subject was provided with visual velocity feedback. The wrist was braced, the elbow was supported by a sling, and the shoulders were strapped to the chair. (b) Representative trial from one subject in the CW direction in the slow conditions: zero-force trajectory (variable color line), path defined by the constraint (black dashed lines).

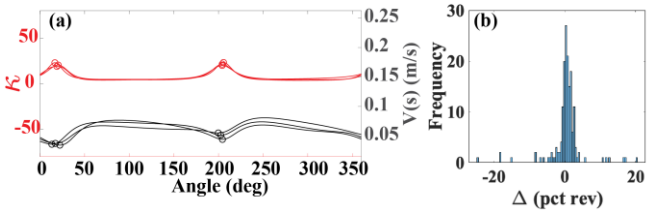

Figure 2: (a) Tangential velocity (V(s)) and curvature (κ) of the zero-force trajectory for a single trial plotted vs. the angle of the circular constraint; successive cycles are superimposed. (b) Histogram of the interval Δ for all trials performed by one subject at the slow speed in the CW direction.

IV. Discussion/Conclusions

Even though the hand was confined to a circular path, when the peripheral biomechanics were subtracted, a velocity-curvature relationship consistent with unconstrained

*Research supported by NSF NRI Grant No.1637824, NIH Grant No. R01-HD087089, and the Eric P. and Evelyn E. Newman Fund. Dagmar Sternad was supported by R01-HD081346, NSF-NRI 1637854, NSF-CRCNS 1723998 and NSF-M3X 1825942.

J. Hermus is with the Department of Mechanical Engineering, Massachusetts Institute of Technology, Cambridge, MA 02139 USA (corresponding author to provide phone: 608-444-2779; (e-mail: jhermus@mit.edu).

D. Sternad is with the Departments of Biology, Electrical & Computer Engineering, and Physics, Northeastern University, Boston, MA 02115 USA

N. Hogan is with the Departments of Brain and Cognitive Sciences and Mechanical Engineering, Massachusetts Institute of Technology, Cambridge, MA 02139 USA

movements was revealed. There was a significant coincidence of curvature and velocity extrema in the zero-force trajectory. This observation was not evident in endpoint Cartesian space, as it was disguised by the interactive dynamic properties of the limb. These findings indicate that movement planning in zero-force space may be similar in unconstrained and constrained motion.

V. Appendix

The model of the human was constructed of the upper arm (link 1), and forearm (f) plus hand (h) (link 2). Each of the body segments was described by the following parameters: length (l), mass (m), inertia (I), radius of gyration (k_a), and center of mass (c). The length l_f was the distance from the elbow to the center of the fist; the length c_h was the distance from the center of the wrist to the center of the hand. The hand was assumed to be a point mass at the end of the forearm.

The model of the arm and crank system was constructed in the same manner as performed by Ohta et al. [7]. displays the variables and notation used in the development of the model. The system has one degree of freedom; therefore, there is a kinematic relationship which can be used to transform from Cartesian position, $\boldsymbol{x} = [x, y]^T$, to joint position, $\boldsymbol{q} = [q_1, q_2]^T$, and to crank position, θ, where the center of the crank is defined as $\boldsymbol{x_c} = [x_c, y_c]$.

$$\boldsymbol{x} = \begin{bmatrix} \mathrm{l_1C_1} + \mathrm{l_2C_{12}} \\ \mathrm{l_1S_1} + \mathrm{l_2S_{12}} \end{bmatrix} = \begin{bmatrix} \mathrm{r}\cos\theta \\ \mathrm{r}\sin\theta \end{bmatrix} + \boldsymbol{x_c} \tag{1}$$

The notation S_1, C_1 denote $\sin(q_1)$, $\cos(q_1)$ and S_{12}, C_{12} denote $\sin(q_1 + q_2)$, $\cos(q_1 + q_2)$. The radius of the crank is r, the damping of the crank is b_c, and the inertia is I. The upper arm denoted 1, and the forearm denoted 2 are described by length l_1, l_2, mass m_1, m_2, inertia about the z axis I_1, I_2, and center of mass distance from the joint axis c_1, c_2. The force on the handle is $\boldsymbol{F} = \left[F_x, F_y\right]^T$, with the normal unit vector, $\boldsymbol{n}$ and tangential unit vector, $\boldsymbol{e}$. The joint torque is denoted $\boldsymbol{\tau} = [\tau_1, \tau_2]^T$.

From the sum of moments acting on the crank,

$$I\ddot{\theta} + b_c\dot{\theta} = r\boldsymbol{e}^T\boldsymbol{F} \tag{2}$$

summation of moments about the shoulder,

$$\boldsymbol{M}\ddot{\boldsymbol{q}} + \boldsymbol{h} = \boldsymbol{\tau} - \boldsymbol{J}^T\boldsymbol{F} \tag{3}$$

and the kinematic relationship that equates the acceleration at the handle to the acceleration at the hand,

$$\ddot{\boldsymbol{x}} = \boldsymbol{J}\ddot{\boldsymbol{q}} + \dot{\boldsymbol{J}}\dot{\boldsymbol{q}} = r(\ddot{\theta}\boldsymbol{e} - \dot{\theta}^2\boldsymbol{n}) \tag{4}$$

and the joint torque was defined by,

$$\boldsymbol{\tau} = \boldsymbol{K}(\boldsymbol{q}_0 - \boldsymbol{q}) + \boldsymbol{B}(\dot{\boldsymbol{q}}_0 - \dot{\boldsymbol{q}}) \tag{5}$$

a model of the system can be constructed. Substituting Equation 5, into Equation 2, 3, and 4 the equation can be manipulated to solve for $\dot{\boldsymbol{q}}_0$.

$$\begin{aligned} &\dot{\boldsymbol{q}}_0 \\ &= \boldsymbol{B}^{-1}\left[\boldsymbol{M}\boldsymbol{J}^{-1}\left[\{\boldsymbol{J}\boldsymbol{M}^{-1}\boldsymbol{J}^T + r^2I^{-1}\boldsymbol{e}\boldsymbol{e}^T\}\boldsymbol{F} - \dot{\boldsymbol{J}}\dot{\boldsymbol{q}}\right.\right. \\ &\left.\left. - r\dot{\theta}\left(\dot{\theta}\boldsymbol{n} + b_cI^{-1}\boldsymbol{e}\right)\right] + \boldsymbol{h} - \boldsymbol{K}(\boldsymbol{q}_0 - \boldsymbol{q})\right] + \dot{\boldsymbol{q}} \end{aligned} \tag{6}$$

Terms comprising these equations include the mass matrix, the centrifugal and Coriolis forces, and the Jacobian relating unconstrained differential arm motions to hand motions.

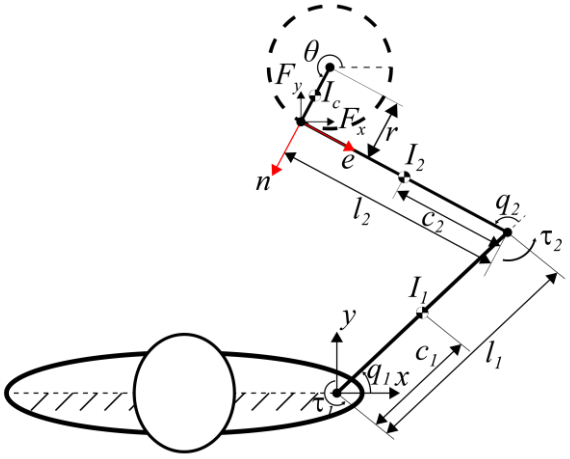

Figure 3: Model of crank rotation task which displays the sign convention and notation used in the computations.

VI. References

[1] F. Lacquaniti, C. Terzuolo, and P. Viviani, "The law relating the kinematic and figural aspects of drawing movements," *Acta Psychol. (Amst).*, vol. 54, no. 1–3, pp. 115–130, Oct. 1983.

[2] W. Abend, E. Bizzi, and P. Morasso, "Human arm trajectory formation," *Brain*, vol. 105, no. Pt 2, p. 331—348, Jun. 1982.

[3] D. Huh and T. J. Sejnowski, "Spectrum of power laws for curved hand movements," *Proc. Natl. Acad. Sci.*, vol. 112, no. 29, pp. E3950–E3958, 2015.

[4] J. T. Massey, J. T. Lurito, G. Pellizzer, and A. P. Georgopoulos, "Three-dimensional drawings in isometric conditions: relation between geometry and kinematics," *Exp. Brain Res.*, vol. 88, no. 3, pp. 685–690, 1992.

[5] A. B. Schwartz, "Direct cortical representation of drawing," *Science (80-.).*, vol. 265, no. 5171, p. 540 LP-542, Jul. 1994.

[6] S. Schaal and D. Sternad, "Origins and violations of the 2/3 power law in rhythmic three-dimensional arm movements," *Exp. Brain Res.*, vol. 136, no. 1, pp. 60–72, Jan. 2001.

[7] K. Ohta, M. M. Svinin, Z. Luo, S. Hosoe, and R. Laboissière, "Optimal trajectory formation of constrained human arm reaching movements," *Biol. Cybern.*, vol. 91, no. 1, pp. 23–36, 2004.